Supporting Information

The Role and Evolutionary Pathway of Spin States in CoFe Prussian blue analogue for Photo-Assisted Water Oxidation Electrocatalysis

Dujie Feng,[a] Yi Zhou,*[a] Wanhong He,*[a] Jin Zhang,[b] Guihua Huang,[a] Yiming Shao[a]

[a]School of Chemistry and Chemical Engineering, Changsha University of Science and Technology, Changsha 410114, P. R. China. E-mail: 008639@csust.edu.cn

[b]School of Traffic and Transportation Engineering, Changsha University of Science and Technology, Changsha 410114, P. R. China.

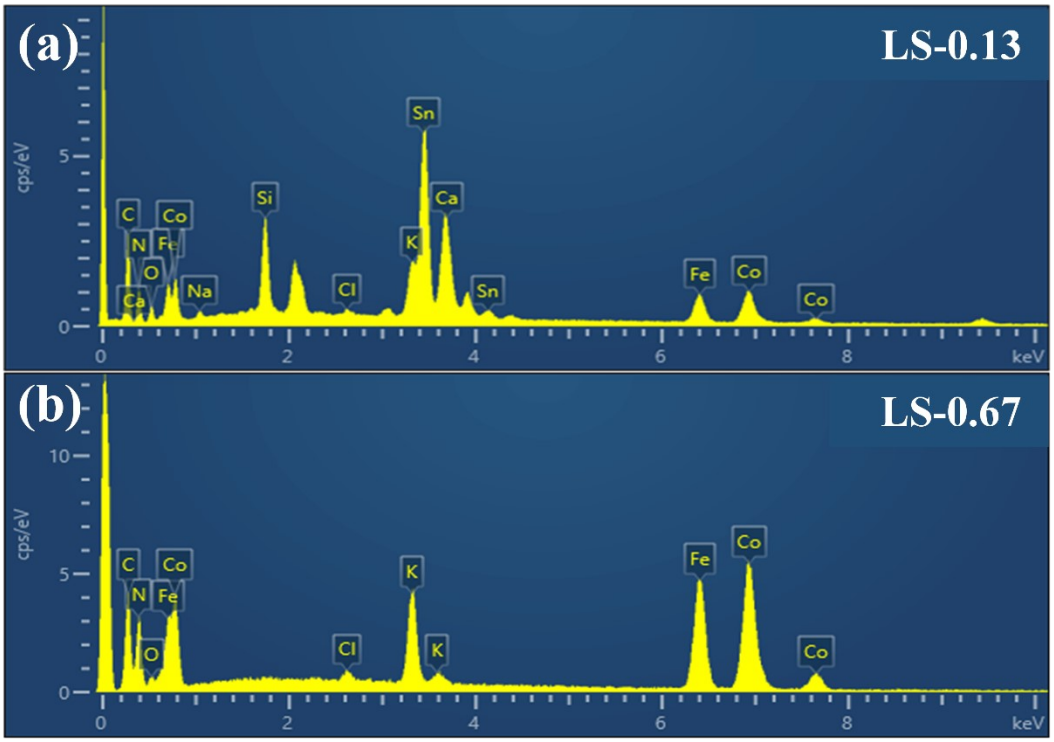

Fig. S1. The EDS profiles of LS-0.13 and LS-0.67.

Table S1. The lattice constant obtained through the Bragg equation

Sample	Lattice constant (Å)
LS-0.13	9.9051±0.0097
LS-0.13-Used	9.8742±0.0036
LS-0.67	9.8633±0.0089
LS-0.67-Used	9.8583±0.0028

Table S2. Results of deconvolution of the vibration absorptions of the CN groups for CoFe PBAs.

Sample	The corresponding spin state	Average center of the peak	The molar ratio of the corresponding spin state
LS-0.13	LS Co^{III}-NC-Fe^{II}	2115.0	13.56%
	Co^{II}-NC-Fe^{II}	2090.0	86.44%
LS-0.13-Used	LS Co^{III}-NC-Fe^{II}	2123.8	33.19%
	Co^{II}-NC-Fe^{II}	2077.6	66.81%
LS-0.67	LS Co^{III}-NC-Fe^{II}	2120.7	67.27%
	Co^{II}-NC-Fe^{II}	2086.5	32.73%
LS-0.67-Used	LS Co^{III}-NC-Fe^{II}	2117.3	30.38%
	Co^{II}-NC-Fe^{II}	2086.5	69.62%

Table S3. The peak information and molar percentages of ions with different oxidation states derived from XPS analysis.

Element		Fe $2p_{3/2}$			Fe $2p_{1/2}$				Co $2p_{3/2}$			Co $2p_{1/2}$			
		Fe^{2+}	Fe^{3+}	sat.	Fe^{2+}	Fe^{3+}	sat.	Co^{3+}	Co^{2+}	sat.	LMM	Co^{3+}	Co^{2+}	sat.	LMM
LS-0.13	Peak position (eV)	708.6	709.9	711.5	721.4	722.7	724.2	780.5	782.6	785.8	789.2	795.7	797.8	800.8	804.3
	molar percentage (%)	46.5	13.1	4.5	23.2	6.6	6.1	5.1	39.7	13.8	9	2.6	19.8	6.2	3.8
LS-0.13-Used	Peak position (eV)	708.6	709.9	712	721.4	722.7	724.1	780.8	782.6	785.1	788.5	795.5	797.6	799.4	802.2
	molar percentage (%)	49.9	11.6	2	24.9	5.8	5.8	7.9	38.8	13.5	8.1	4	19.4	6	2.3
LS-0.67	Peak position (eV)	708.5	709.7	711.8	721.3	722.6	723.9	780.6	782.6	785.6	789.1	795.8	797.8	800.4	804.5
	molar percentage (%)	53.4	7.9	2.1	26.7	4	6	14.9	33.6	12.4	8.7	7.4	16.8	4	2.2
LS-0.67-Used	Peak position (eV)	708.5	710	711.8	721.3	722.8	724.2	780.8	782.6	785.6	788.8	795	797.6	800.1	803.6
	molar percentage (%)	46.4	11.4	6.5	23.2	5.7	6.8	7.4	36.3	14.8	9.7	3.7	18.2	6.4	3.5

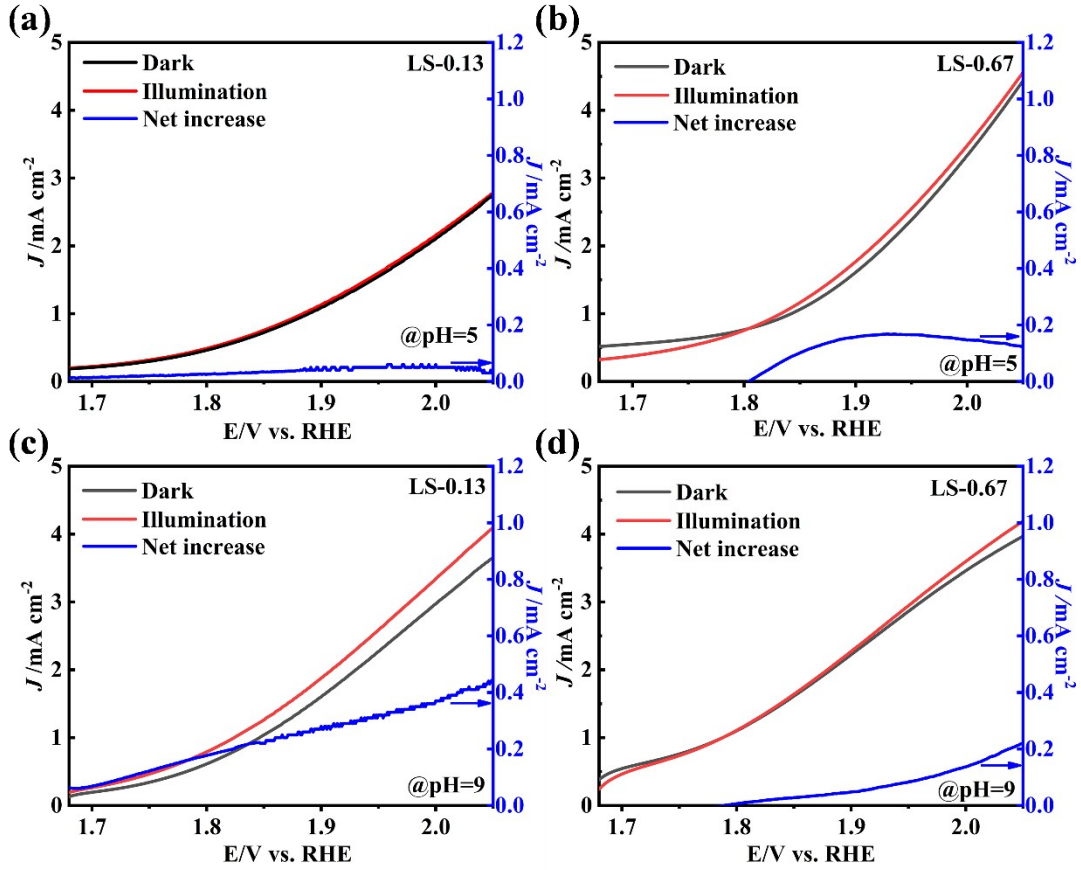

Fig. S2 LSV curves and net photocurrent density for (a, c) LS-0.13 and (b, d) LS-0.67 at different pH values.

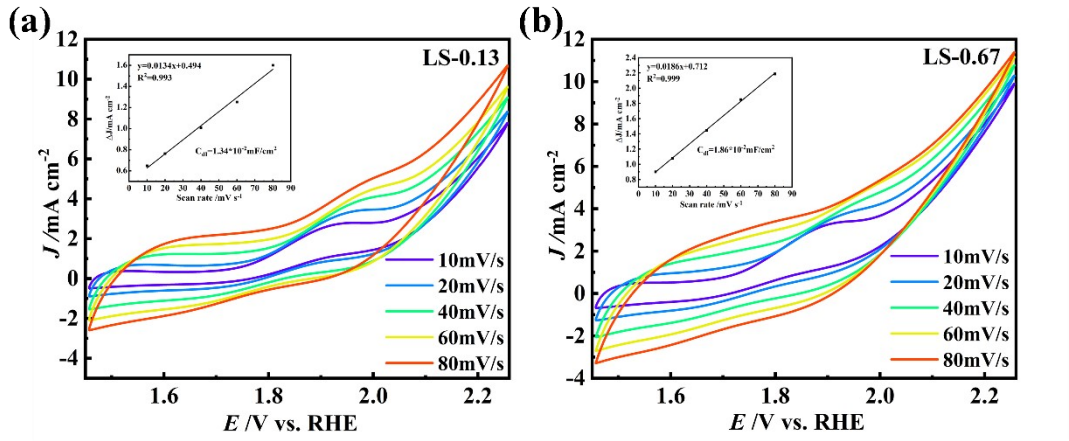

Fig. S3. Cyclic voltammograms and double-layer capacitance plots of (a) LS-0.13 and (b) LS-0.67 at different scan rates in a 0.1 M KPi + 1 M KNO_3 electrolyte at pH=7.

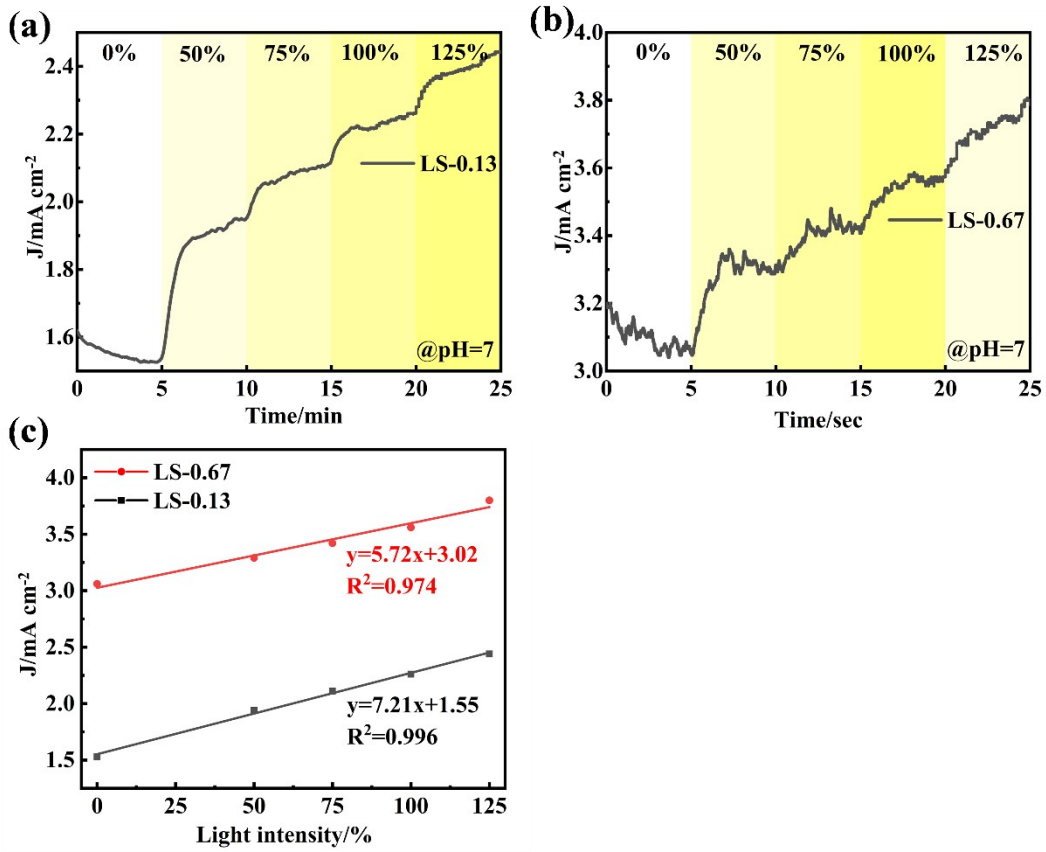

Fig. S4. The CA curves of(a) LS-0.13 and (b) LS-0.67 under a constant voltage of 2.0 V vs. RHE, with increasing light intensity at an interval of 300 s. (c) The linear relationship between light intensity and current density.

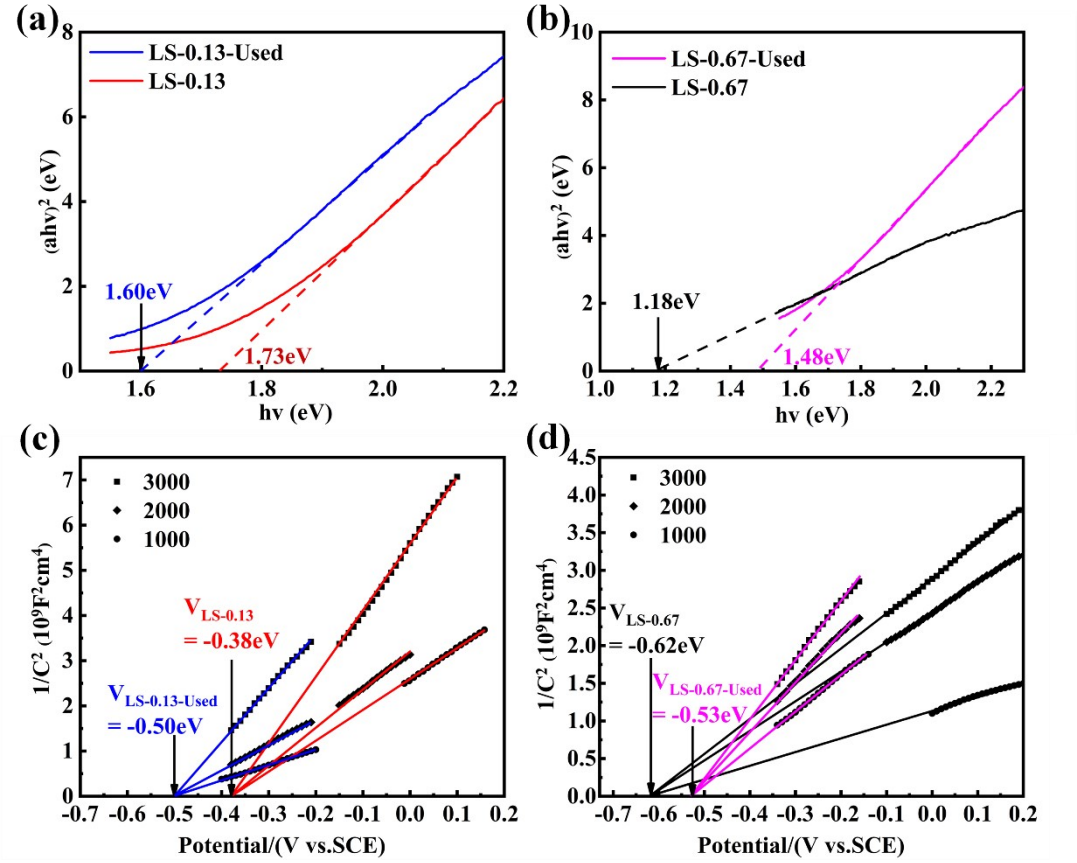

Fig. S5. (a, b) Energy band gap and (c, d) Mott-Schottky plots of CoFe PBAs with different LS ratio pre- and post-photo-assisted OER process.

Table S4. The band structure data of CoFe PBAs.

Sample	E_g	V_{fb} vs. SCE	V_{fb} vs. RHE	E_{CB}	E_{VB}
LS-0.13	1.73	-0.38	0.28	0.18	1.91
LS-0.13-Used	1.60	-0.50	0.16	0.06	1.66
LS-0.67	1.18	-0.62	0.04	-0.06	1.12
LS-0.67-Used	1.48	-0.53	0.13	0.03	1.51

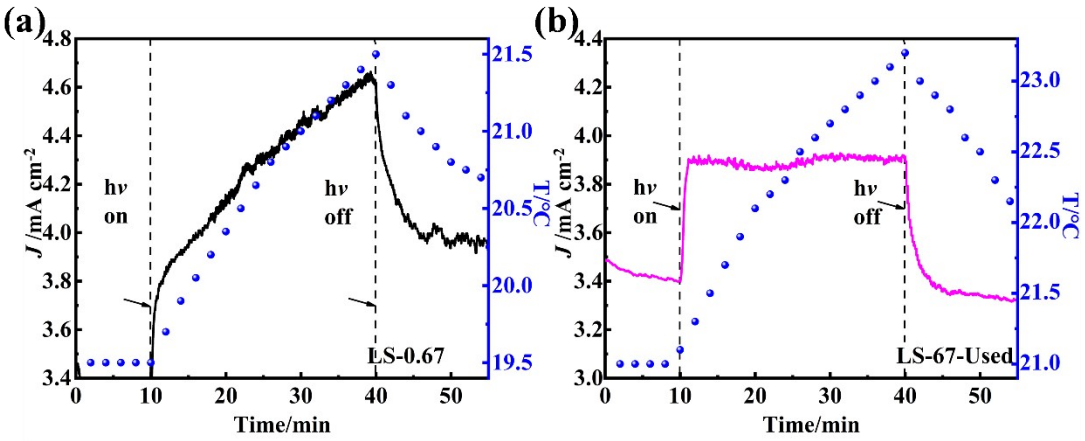

Fig. S6. Comparison of the change of temperature and the current density profiles for (a) LS-0.67 and (b) LS-0.67-Used. The measurements were conducted at 2.0 V vs. RHE, in a 0.1 M KPi + 1 M KNO_3 electrolyte at pH 7. The electrodes were irradiated by a 100 mW·cm^{-2} Xenon light for 30 min. For both as-prepared LS-0.67 and LS-0.67-Used, the changes in the temperature-time curve and the I-t curve showed different trends. In the light-on stage, the current density of LS-0.67 increased rapidly in the very beginning, but the temperature increased gradually during the whole stage. Upon turning off the light, the current density of LS-0.67 decreased fast in the first 5 min and then decayed very slowly, while the temperature decreased approximately linearly. For LS-0.67-Used, the current density kept constantly during the light irradiation stage whereas the temperature kept increasing. After turning off the light, the current density of LS-0.67-Used dropped rapidly while the temperature decreased linearly. Thus, the experiments indicate that the thermal effect had little impact on the current density.